USP22 promotes pro-inflammatory responses in *Pseudomonas aeruginosa*-induced keratitis by targeting TRAF6

DI CHEN[1], DAWEI SONG[2], YIBIN MA[2], WEIZHAO LU[3], JIANFENG QIU[3] and YI WANG[4]

[1]Department of Ophthalmology, Second Affiliated Hospital of Shandong First Medical University and Shandong Academy of Medical Sciences, Tai'an, Shandong 271000; [2]Department of Ophthalmology, Tai'an City Central Hospital, Tai'an, Shandong 271000; Departments of [3]Radiology and [4]Ophthalmology, Shandong First Medical University and Shandong Academy of Medical Sciences, Tai'an, Shandong 271000, P.R. China

Abstract. *Pseudomonas aeruginosa* (PA)-induced keratitis is characterized by inflammatory epithelial edema, stromal infiltration, corneal ulceration and can lead to vision loss. The present study aimed to study the effect of ubiquitin-specific protease 22 (USP22) on PA-induced keratitis. Using RT-qPCR and western blotting, significantly increased expression of USP22 was identified in mouse corneas and cultured RAW264.7 cells following PA stimulation. In addition, the results of *in vivo* experiments, western blot assay and ELISA suggested that the silencing of USP22 attenuated disease progression, downregulated the NF-κB pathway and suppressed the expression of pro-inflammatory cytokines following PA stimulation. Notably, it was identified that the expression of tumor necrosis factor receptor-associated factor 6 (TRAF6) was decreased by silencing of USP22 and USP22 was found to remove lysine 48-linked poly-ubiquitination chains from TRAF6 to stabilize TRAF6 expression and these effects were clearly aggravated following PA infection.

Introduction

Pseudomonas aeruginosa (PA) is the pathogen most commonly associated with the use of contact lenses (1). PA keratitis is a rapidly developing and destructive ophthalmic disease, which can lead to ulcer, corneal perforation and even severe vision loss (2). Despite the rapid progress of modern medicine, there is still a lack of effective treatment for PA keratitis (3). It is necessary to identify novel therapeutic targets for PA keratitis. Therefore, keeping the immune homeostasis and regulating the inflammatory immune response of the eyes are the theme of the present study.

Ubiquitination and de-ubiquitination processes have been reported to maintain the stability of a large number of critical proteins and internal environment and participate in the regulation of important physiological processes (4). When the ubiquitination chain of lysine 63 is formed, the activity and other functions of the substrates are changed (5). If the substrate is modified by lysine 48 (K48) ubiquitin, the target protein is degraded by proteasome system (6). Recently, studies have demonstrated that the ubiquitination process is crucial for the regulation of inflammatory responses in PA-induced keratitis (7,8).

Deubiquitinating enzymes (DUBs) are proteases that process ubiquitin or ubiquitin-like gene products and reverse the modification of proteins by a single ubiquitin (9). Ubiquitin-specific proteases (USPs) are the largest subclass of DUBs with specific targets (10). Ubiquitin-specific protease 22 (USP22) is a member of USPs in mammals and contains an N-terminal zinc-finger domain for substrate interaction and a C-terminal ubiquitin-specific peptidase domain for protein deubiquitination (11). Its expression level is related to tumor metastasis, drug resistance and cell cycle progress and is crucial in the process of tumor oncogenesis and development; it is therefore considered a biomarker and treatment target of tumors (12). However, no studies, to the best of the authors' knowledge, have documented the role of USP22 in PA-induced keratitis.

The present study demonstrated that the expression of USP22 was increased by PA infection. Silencing of USP22 significantly delayed the disease progression of PA-mediated keratitis and attenuated pro-inflammatory cytokines production induced by PA infection. Knockdown of USP22 expression suppressed NF-κB activation and enhanced K48-linked polyubiquitination level of TRAF6. These results indicated that USP22 is a positive regulator of pro-inflammatory responses in PA-induced keratitis.

Correspondence to: Dr Yi Wang, Department of Ophthalmology, Shandong First Medical University and Shandong Academy of Medical Sciences, 619 Changcheng Road, Tai'an, Shandong 271000, P.R. China
E-mail: wangyi_sdtaian@126.com

Dr Jianfeng Qiu, Department of Radiology, Shandong First Medical University and Shandong Academy of Medical Sciences, 619 Changcheng Road, Tai'an, Shandong 271000, P.R. China
E-mail: jfqiu_sdtaian@126.com

Materials and methods

Cell culture. Mouse macrophage cell line RAW264.7 was obtained from American Type Culture Collection and the cells grown in DMEM medium (HyClone; Cytiva) containing 10% FBS (HyClone; Cytiva), 100 U/ml penicillin (HyClone; Cytiva) and 100 μg/ml streptomycin (HyClone; Cytiva) at 37˚C under 5% CO_2.

Experimental infection with PA. Wild-type (WT) 8-week-old female C57BL/6J mice (18-22 g, n=90) were purchased from Beijing Vital River Laboratory Animal Technology Co., Ltd. The mice were maintained in a specific pathogen-free grade animal facility at room temperature and humidity (50-60%) under a 12-h light/dark cycle and were allowed free access to standard mouse chow and water. The experiments were carried out according to the National Institutes of Health Guide for the Care and Use of Laboratory Animals (NIH publication, no. 85-23, revised 2011) (13), approved by the Animal Ethics Committee of the Scientific Investigation Board of Shandong First Medical University and performed as previous reported (7). Mice were intubated and anaesthetized with mechanical ventilation using 2-3% isoflurane. Anesthesia was maintained by inhalation of 1-2% isoflurane in 100% oxygen. The adequacy of anaesthesia and mortality of mice were monitored by measuring heart rate and the response to tail stimulation. In order to maintain the body temperature of mice at 37˚C, a layer of water circulating at constant temperature was arranged on the experimental platform. Following anesthesia with isoflurane, three 1-mm incisions were made on the left cornea with sterile 25 gauge needle. A bacterial suspension (5 μl) containing 1×10^6 colony-forming units (CFUs) of PA ATCC strain 19660 was used locally on the ocular surface. The eyes were examined at 24 h or other time points following the infection to ensure that the mice were infected and to monitor the disease. For euthanasia, the mice were treated with pentobarbital (150 mg/kg, administered intraperitoneally; Sigma-Aldrich; Merck KGaA) followed by cervical dislocation in accordance with NIH guidelines for the humane treatment of animals. All efforts were made to minimize suffering. In the experiment, there was no mortality of mice due to human operations. The corneal disease was graded as follows: 0, clear or slight opacity partially or fully covering the pupil; +1, slight opacity partially or fully covering the anterior segment; +2, dense opacity partially or fully covering the pupil; +3, dense opacity covering the entire anterior segment; and +4, corneal perforation or phthisis.

Bacterial plate counts. Subsequently, 5 days after infection, the corneas (n=5/group/time point) were collected and the number of viable bacteria was counted as previously reported (14). In brief, the cornea was homogenized in sterile water containing 0.85% (w/v) NaCl and 0.25% BSA (Sigma-Aldrich; Merck KGaA). The 10-fold diluent of the sample was coated on the Pseudomonas Isolation Agar (Difco; Becton, Dickinson and Company) for three times followed by the incubation overnight at 37˚C. The data were reported as 105 CFU per cornea ± standard deviation.

Histology. Eyes were collected and fixed in 10% neutral buffered formalin for 24 h at room temperature. (Sigma-Aldrich;

Merck KGaA) 5 days after PA infection. The eye tissues were embedded in paraffin and anterior sections (8 μm) of the corneal epithelium were cut serially, mounted on adhesive glass slides and stained by hematoxylin (cat. no. C0105M-1; Beyotime Institute of Biotechnology; 3 min) and eosin (cat. no. C0105M-2; Beyotime Institute of Biotechnology; 15 sec) at room temperature. All sections were visualized with a laser scanning confocal microscope (LSM700; Carl Zeiss AG).

Lentivirus preparation and infection. Lentivirus (BLOCK-iT™ Lentiviral RNAi Expression System; cat. no K4944-00; Invitrogen; Thermo Fisher Scientific, Inc.) containing control plasmid (sequence: 5'-AUUGUCAUCACCUUUGCAGTT -3') or short hairpin (sh)RNA targeting USP22 (sequence: 5'-CGUCAAAGGUGAUGACAAUTT-3') constructed by MDL Biotech, was used according to the manufacturer's protocols. shRNA lentivirus was packaged and titered in 293T cells (obtained from American Type Culture Collection) and the enriched lentivirus particles were used for cell infection at 50 multiplicities of infection in the presence of polybrene. For *in vivo* infection, the protocol was performed as previously described (8). Lentiviruses were subconjunctivally injected into the left eye of C57BL/6J mice (5 μl/mouse at a viral titer of 1×10^8) once a week for three times before PA infection.

Reverse transcription-quantitative (RT-q) PCR. Cells (1×10^4 cells/well) were cultured to 90% confluence in 6-well plates before RNA extraction. Total RNA was extracted using the TRIzol® reagent according to the manufacturer's instructions (Thermo Fisher Scientific, Inc.). Equal volumes of RNA samples (1.0 μg) were collected and the first strand of cDNAs was synthesized using TaqMan™ Reverse Transcription Reagents (Thermo Fisher Scientific, Inc.) according to the manufacturer's instructions. A LightCycler (ABI PRISM 7000; Applied Biosciences) and a SYBR RT-PCR kit (Takara Biotechnology Co., Ltd.) were used for RT-qPCR according to the manufacturer's instructions (25 μl reaction volume). GAPDH was used as the internal control and the thermocycling conditions were 1 cycle (95˚C for 5 min) and 40 cycles (95˚C for 15 sec, 56˚C for 30 sec and 72˚C for 30 sec). The $2^{-\Delta\Delta Cq}$ method was used to evaluate the relative quantities of each amplified product in the samples (15). Primer sequences used in qPCR are given in Table I. The data are representative of three biological replicates.

ELISA analysis. For *in vitro* experiments, the supernatants were collected following PA infection for ELISA analysis. For *in vivo* experiments, the corneas were individually collected following PA infection for 5 days and then homogenized in 0.5 ml of PBS with 0.1% Tween-20. The levels of IL-6 (cat no. M6000B), TNF-α (cat no. MTA00B) and matrix metallo-proteinase 1 (cat no. DY901B) were measured by ELISA kits (R&D Systems) in accordance with the manufacturer's instructions.

Western blot analysis. The protocols were performed as described previously (8). The cells or corneas were lysed using RIPA buffer (MDL Biotech) and total protein in the supernatants was quantified using a Bio-Rad quantification assay (Bio-Rad Laboratories, Inc.). Equal amounts of

Table I. List of primers used.

Gene	Sequence (5'-3')
USP22	F: CCTGCACGTTTTCGTGGAAC
	R: TCTCCACGATGTTGGTGAGC
TNF-α	F: GCCACCACGCTCTTCTGTCT
	R: TGAGGGTCTGGGCCATAGAAC
IL-1β	F: ACCTTCCAGGATGAGGACATGA
	R: AACGTCACACACCAGCAGGTTA
IL-6	F: ACAACCACGGCCTTCCCTAC
	R: CATTTCCACGATTTCCCAGA
GAPDH	F: AATGACCCCTTCATTGAC
	R: TCCACGACGTACTCAGCGC

F, forward; R, reverse.

protein (25 μg) was loaded on 10% sodium dodecyl sulfate polyacrylamide gel electrophoresis and then transferred onto a PVDF membrane (EMD Millipore) followed by blocking with 2.5% nonfat dry milk for 1 h at room temperature. Antibodies for USP22 (1:1,000; cat. no. ab195289; Abcam), K48-linked ubiquitin (linkage-specific K48, 1:800; cat. no. ab140601; Abcam), TRAF6 (1:1,000; cat. no. ab33915; Abcam) and the antibodies specific for p65 (1:800; cat. no. 8242; Cell Signaling Technology Inc.), phosphorylated (p-)p65 (1:800; cat. no. 3033, Cell Signaling Technology Inc.), IκBα (1:800; cat. no. 4814; Cell Signaling Technology Inc.), p-IκBα (1:800; cat. no. 2859; Cell Signaling Technology Inc.) and β-actin (1:2,000; cat. no. sc58673; Santa Cruz Biotechnology, Inc.) were added and the membrane incubated overnight at 4˚C. Subsequently, the membrane was incubated with the corresponding horseradish peroxidase-conjugated secondary antibody (goat anti-rabbit IgG; cat. no. sc-2004; 1:2,000; Santa Cruz Biotechnology, Inc. and goat anti-mouse IgG; cat. no. sc-2005; 1:2,000; Santa Cruz Biotechnology, Inc.) and detected with enhanced chemiluminescence (Thermo Fisher Scientific, Inc.). Protein brands were detected and with Bio-Rad ChemiDoc™ XRS+ System (Bio-Rad Laboratories, Inc.) and analyzed with Image Lab software (v4.1; Bio-Rad Laboratories, Inc.).

Immunoprecipitation and ubiquitination. Following PA infection for the indicated time points, RAW264.7 cells were lysed with co-IP lysis buffer [150 mM NaCl, 20 mM Tris-HCl, pH 7.4, 1% Triton X-100 and 1 mM EDTA supplemented with protease inhibitor cocktail (cat. no. 04693132001, Roche Applied Sciences)]. The cell lysates (5 mg protein) were subjected to immunoprecipitation with the appropriate antibodies (TRAF6; 1:500; cat. no. ab33915; Abcam and IgG; 1:500; cat. no. ab6708; Abcam) overnight at 4˚C and then incubated with protein A/G Plus-Agarose (cat. no. sc-2003; Santa Cruz Biotechnology, Inc.) for 12 h at 4˚C. The beads were washed with the lysis buffer 3 times by centrifugation at 300 x g for 10 min at 4˚C. The immunoprecipitated proteins were separated by 10% SDS-PAGE followed by immunoblotting with the appropriate antibodies (USP22; 1:1,000; cat. no. ab195289; Abcam, TRAF6, 1:1,000; cat. no. ab33915; Abcam, β-actin; 1:2,000; cat. no. sc58673; Santa

Cruz Biotechnology, Inc.). The ubiquitination of TRAF6 was detected as described previously (8). Briefly, following treatment, the cells were harvested and lysed with buffer (50 mM Tris, 140 mM NaCl, 1% SDS). Samples were boiled for 5 min and then diluted 10-fold with co-IP lysis buffer. Following centrifugation (300 x g for 10 min at 4˚C), the supernatants were incubated with anti-TRAF6 antibody (1:500; cat. no. ab33915; Abcam) overnight at 4˚C and then incubated with protein A/G Plus-Agarose (cat. no. sc-2003; Santa Cruz Biotechnology, Inc.) for 12 h at 4˚C, followed by immunoprecipitation assay and western blot analysis.

Statistical analysis. The differences in clinical score between lentivirus treated corneas were tested by the Mann-Whitney U test at indicated days following infection. One-way ANOVA was performed to compare three or more groups. If the ANOVA analysis was significant, the Tukey's post-hoc test was applied for comparison between each two groups. The other assays were determined by an unpaired, two-tailed Student's t test. $P<0.05$ was considered to indicate a statistically significant difference.

Results

USP22 expression is increased in mouse corneas and in in vitro cultured macrophages following PA infection. In order to illustrate the function of USP22 in PA-induced keratitis, the expression of USP22 following PA infection was first examined. As demonstrated in Fig. 1A and B, the mRNA and protein levels of USP22 were increased in mice corneas following PA stimulation. Following PA infection in corneas, macrophages and other inflammatory cells would infiltrate in the corneal stroma to attack the bacteria (16). The level of USP22 in cultured RAW264.7 cells was detected. Consistently, mRNA and protein levels of USP22 were significantly upregulated by PA stimulation (Fig. 1C and D).

Silencing of USP22 delays the disease progression of PA-induced keratitis. Lentivirus containing USP22 shRNA plasmid was used to knockdown the expression of USP22. C57BL/6 mice were subconjunctivally injected with shRNA-control lentivirus or shRNA-USP22 lentivirus, followed by PA infection. The decreased expression of USP22 in mice corneas was confirmed by RT-qPCR and western blotting (Fig. 2A). The clinical scores of PA-infected corneas were next examined and it was found that knocking down the expression of USP22 significantly attenuated PA-induced disease severity (Fig. 2B). In accordance, as demonstrated in Fig. 2C, the bacterial load was markedly decreased in USP22-silenced mice corneas following PA infection. In addition, hematoxylin and eosin staining results demonstrated alleviated inflammation and less infiltration of immune cells in USP22-silenced corneas (Fig. 2D).

Silencing of USP22 suppresses PA-induced pro-inflammatory cytokines production. Inflammatory reaction and pro-inflammatory cytokines production are critical processes in response to PA infection in corneas. Therefore the pro-inflammatory cytokines production in mice corneas and RAW264.7 cells was detected following PA stimulation. As demonstrated in
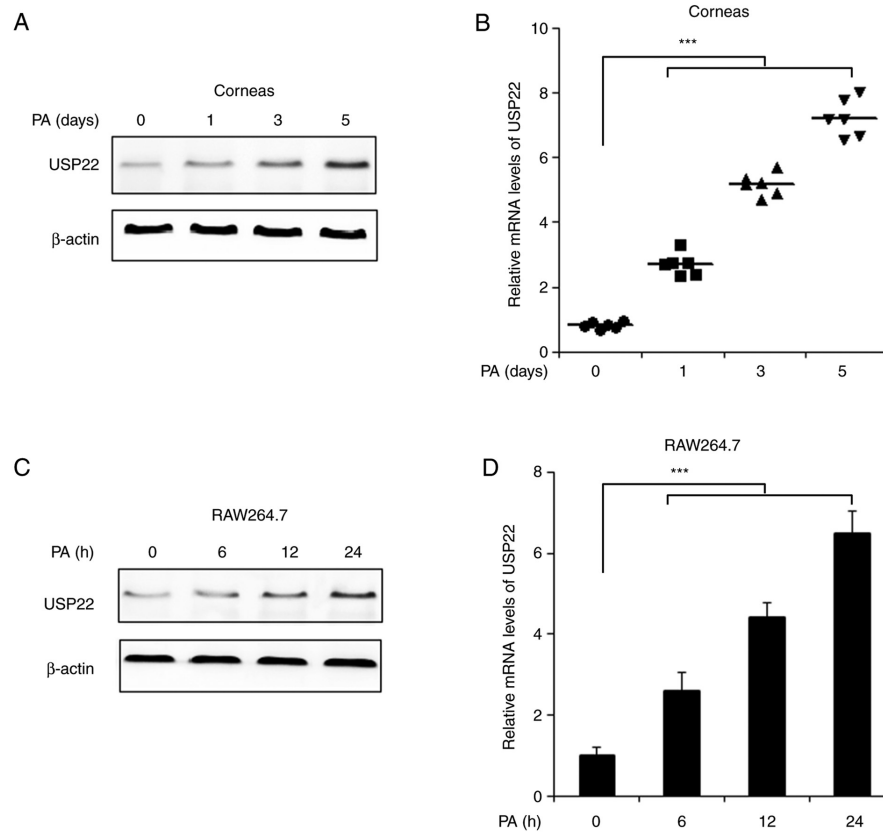
Figure 1. USP22 expression is increased in mouse corneas and *in vitro* cultured macrophages following PA infection. (A) Mouse corneas were infected with PA for the indicated time points, 3 mice/time point, and the protein levels of USP22 were detected. (B) Mouse corneas were infected with PA for indicated time point, 6 mice/time point and USP22 mRNA expression was examined. (C) RAW264.7 cells were infected with PA for indicated time point and the protein levels of USP22 were detected. (D) RAW264.7 cells were infected with PA for indicated time point and USP22 mRNA levels were detected. Data are representative of three independent experiments (mean ± standard deviation). ***$P<0.001$. USP22, ubiquitin-specific protease 22; PA, *Pseudomonas aeruginosa*.
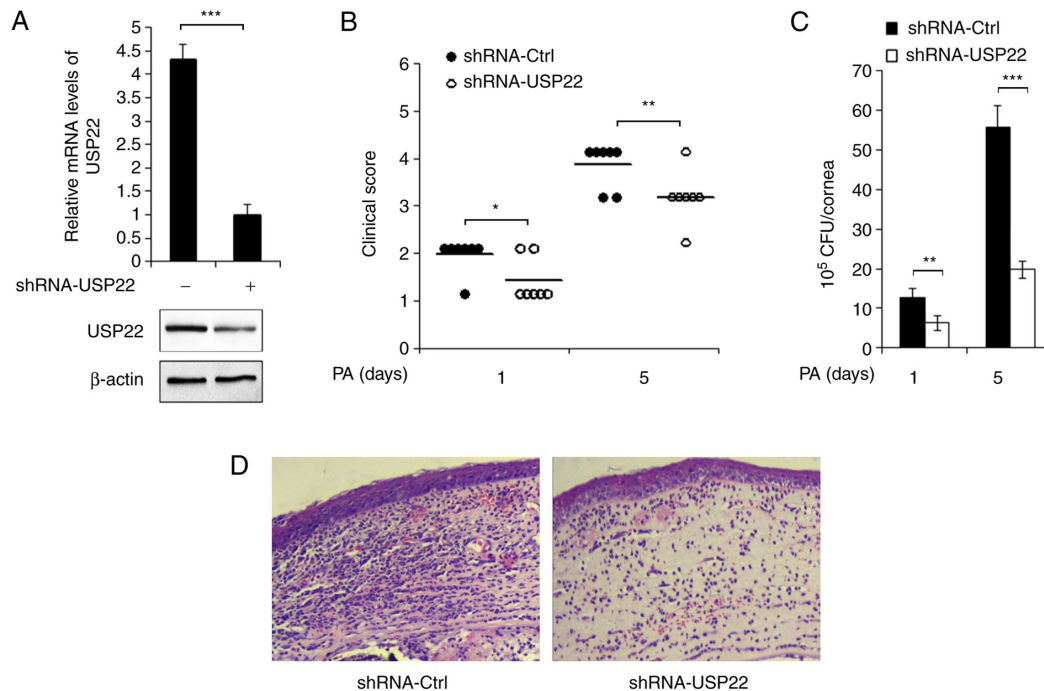

Figure 2. Silencing of USP22 delays the disease progression of PA-induced keratitis. (A) Mouse corneas were infected with shRNA-control lentivirus or shRNA-USP22 lentivirus followed by PA infection for 5 days and the efficiency of shRNAs confirmed, 3 mice/group. (B) Mouse corneas were infected with shRNA-control-lentivirus or shRNA-USP22-lentivirus followed by PA infection for 5 days and clinical scores were recorded, 7 mice/group. (C) Bacterial load in Fig. 1B. (D) Hematoxylin and eosin staining results of infected eyes at 5 days post infection, 3 mice/group; magnification, x100. Data are representative of three independent experiments (mean ± standard deviation). *$P<0.05$; **$P<0.01$; ***$P<0.001$. USP22, ubiquitin-specific protease 22; PA, *Pseudomonas aeruginosa*; sh, short hairpin; Ctrl, control; CFU, colony-forming units.
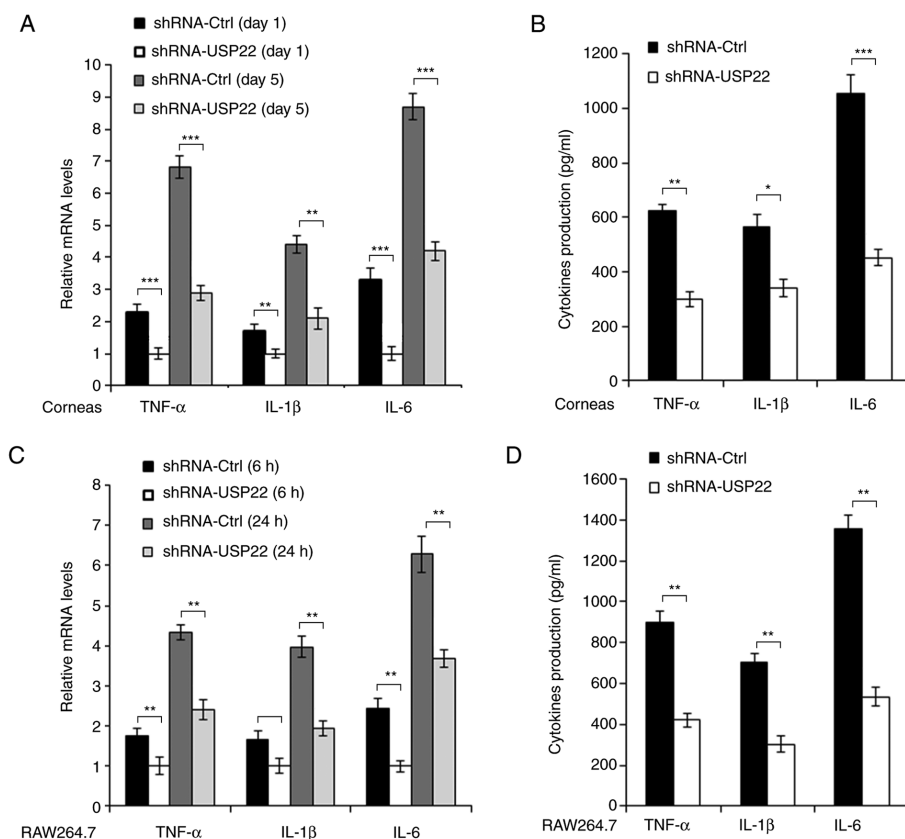
Figure 3. Silencing of USP22 suppresses PA-induced pro-inflammatory cytokines production. USP22 expression in mice corneas was decreased by shRNA-USP22-lentivirus followed by PA stimulation (A) the mRNA expression levels of TNF-α, IL-1β and IL-6 were examined by reverse transcription-quantitative (RT-q) PCR and (B) the protein levels determined by western blotting, 3 mice/group. (C and D) Similar results were observed in RAW264.7 cells. Data are representative of three independent experiments (mean ± standard deviation). $^*P<0.05$; $^{**}P<0.01$; $^{***}P<0.001$. USP22, ubiquitin-specific protease 22; PA, *Pseudomonas aeruginosa*; sh, short hairpin; Ctrl, control.

Fig. 3A and B, mRNA and protein levels of pro-inflammatory cytokines such as TNF-α, IL-1β and IL-6 were decreased in USP22-shRNA-treated mice corneas following PA infection. Similar results were also observed in RAW264.7 cells (Fig. 3C and D).

Silencing of USP22 inhibits NF-κB activation. Production of pro-inflammatory cytokines depends mainly on the NF-κB activation in response to PA infection, so it was hypothesized that USP22 could affect NF-κB activation in PA-infected macrophages. As demonstrated in Fig. 4A-C, the present study found that silencing of USP22 greatly suppressed phosphorylation of p65 and IκBα in RAW264.7 cells infected with shRNA-USP22 lentivirus.

Silencing of USP22 aggravates K48-linked polyubiquitination of TRAF6. TRAF6 is reported to be an important adaptor of the NF-κB signaling pathway (17), so the present study investigated the relationship between USP22 and TRAF6 by examining the protein level of TRAF6 in USP22-silenced RAW264.7 cells following PA infection. It was found that knockdown of USP22 expression decreased TRAF6 expression in control and PA-treated macrophages (Fig. 5A). Furthermore, the interaction between USP22 and TRAF6 was observed following PA infection (Fig. 5B). Notably, silencing of USP22 enhanced K48-linked polyubiquitination of TRAF6, especially in PA infected RAW264.7 cells (Fig. 5C).

Discussion

The current study demonstrated the expression of USP22 and its role in PA-induced keratitis. To the best of the authors' knowledge, this is the first report on the relationship between USP22 and PA keratitis.

PA keratitis accounts for ~75% of reported cases of contact lens-associated diseases (14). The pathogenesis of PA keratitis is complex and has a number of factors including bacterial factors and host components. For example, PA can produce a variety of toxic factors, such as exotoxin A, lipopolysaccharide endotoxin and exoenzyme ExoU to induce host cell death (18). In addition, as the critical cells of host immune response, macrophages and monocytes accumulate in the infected area during PA infection (19). The pro-inflammatory cytokines, such as TNF-α, IL-1β and IL-6, are produced by macrophages and monocytes to clear up the bacterial infection, but if not properly controlled, these inflammatory cytokines can aggravate tissue damage, even leading to corneal perforation (20). The current study demonstrated that knocking down the expression of USP22 could delay PA keratitis progression and decrease PA bacterial load, indicating that USP22 is a positive regulator of PA keratitis. As the present study demonstrated, USP22 expression is markedly increased by PA infection in mice corneas and *in vitro* cultured RAW264.7 cells, which suggested that USP22 expression was regulated by PA and that PA keratitis tends to be aggravated with the accumulation of USP22. It
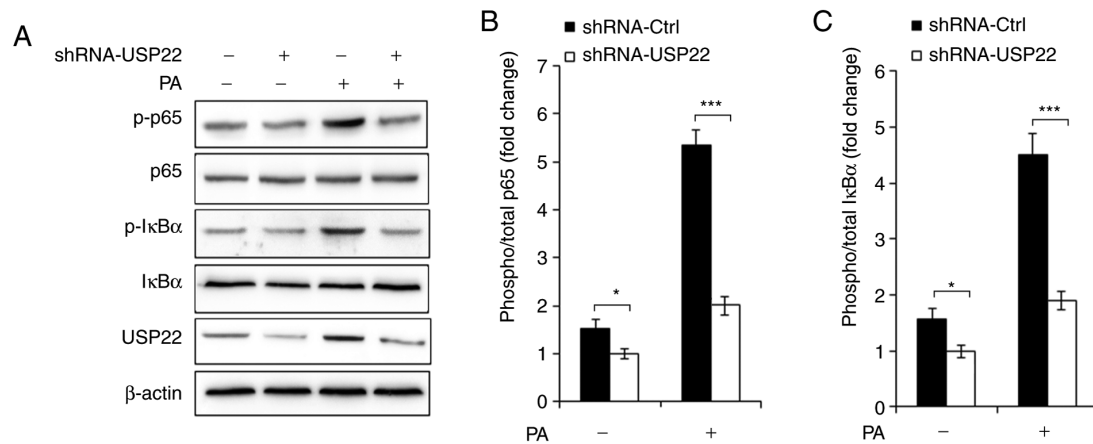
Figure 4. Silencing of USP22 inhibits NF-κB activation. USP22 expression was silenced, followed by PA infection for 24 h. (A) The phosphorylation of p65 and IκBα were examined. Quantification of protein level of (B) p-p65 and (C) IκBα in Fig. 4A. Data are representative of three independent experiments (mean ± standard deviation). *P<0.05; ***P<0.001. USP22, ubiquitin-specific protease 22; PA, *Pseudomonas aeruginosa*; sh, short hairpin; Ctrl, control.
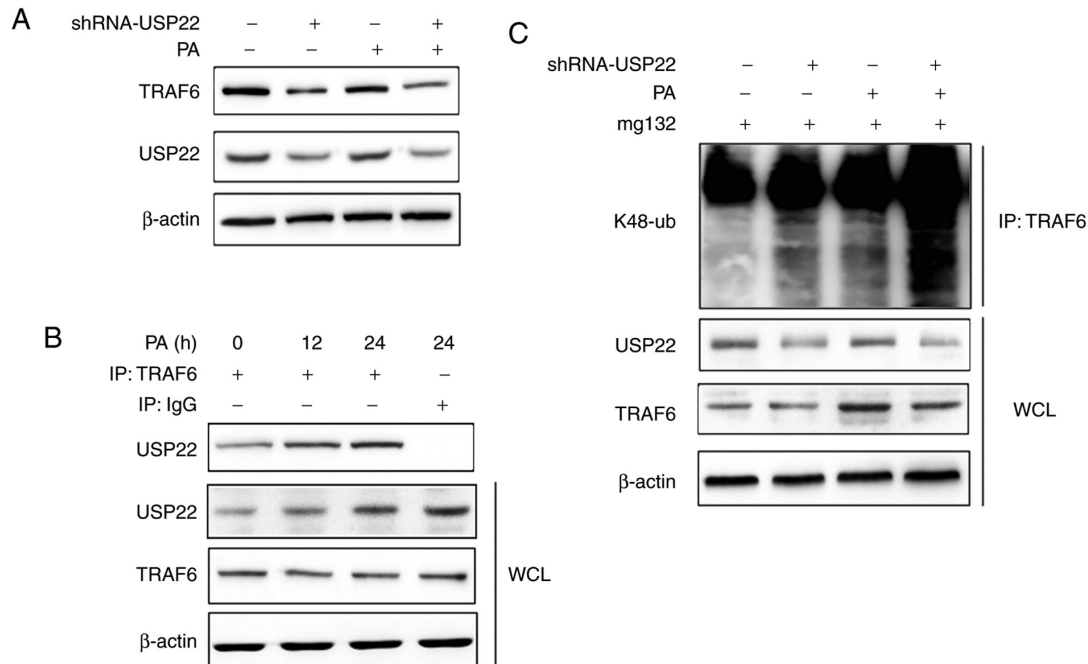

Figure 5. Silencing of USP22 aggravates K48-linked polyubiquitination of TRAF6. (A) TRAF6 expression was examined in USP22-silenced RAW264.7 cells at 24 h following PA infection. (B) Interaction between USP22 and TRAF6 in RAW264.7 cells following PA infection. (C) K48-linked polyubiquitination of TRAF6 in (Fig. 5A) was detected by western blot analysis. Data are representative of three independent experiments (mean ± standard deviation). USP22, ubiquitin-specific protease 22; K48, lysine 48; TRAF6, tumor necrosis factor receptor-associated factor 6; mg132, carbobenzoxy-L-leucyl-L-leucyl-L-leucinal; IP, immunoprecipitation; WCL, whole cell lysate.

was found that silencing of USP22 suppressed production of pro-inflammatory cytokines in PA-infected RAW264.7 cells; these data suggested USP22 as a pro-inflammatory regulator following PA infection.

The NF-κB signaling pathway is widely studied as a paradigm for signal transduction and pro-inflammatory cytokines production (21). Previous studies have reported that the NF-κB signaling pathway serves a crucial role in the development of bacterial keratitis (22-24). The current study identified that silencing of USP22 suppressed phosphorylation levels of p65 and IκBα, which indicated that USP22 could promote NF-κB activation, thereby increasing the expression of pro-inflammatory cytokines.

Ubiquitination modification has been reported to serve crucial roles in NF-κB activation and previous studies have demonstrated that ubiquitination regulation is essential for the regulation of progression of PA keratitis (7,8). In addition, the present study found that USP22 could remove the K48-linked polyubiquitination chain of TRAF6, which is the key adaptor of the NF-κB signaling pathway, leading to the stability of TRAF6 and thereby the promotion of NF-κB activation and the production of downstream pro-inflammatory cytokines.

USP22 is a novel deubiquitinating enzyme and is considered to be important in a number of physiological and pathological processes such as cell cycle, cell proliferation and tumor invasion (25-27). However, the function of USP22 in PA

keratitis remains to be elucidated. The present study detected the level of USP22 in PA-infected mice corneas and RAW264.7 cells and identified that USP22 expression was induced by PA infection. Furthermore, USP22 promoted disease progression of PA keratitis, together with the increased production of pro-inflammatory cytokines. USP22 enhanced PA-induced NF-κB activation and stabilized TRAF6 expression by removing K48-linked polyubiquitination of TRAF6. These findings extended our understanding of the physiological function of USP22 and suggested USP22 is a possible medical target for the treatment of PA keratitis.

However, there were still some limitations in this study. For example, the detection of NF-κB and TRAF6 activity in animal models is still insufficient and the use of human cornea for experiments remains lacking. This will be improved in future studies and the functional research of USP22 in human tissues expanded.

Availability of data and materials

The datasets used and/or analyzed during the current study are available from the corresponding author on reasonable request.

Authors' contributions

DC and YW designed the present study. DC, DS and JQ performed the experiments, collecting data and drafted the manuscript. YM and WL performed the cell experiments and analyzed the data. DC and YW confirm the authenticity of all the raw data. All authors read and approved the final manuscript.

Ethics approval and consent to participate

The experiments were carried out according to the National Institutes of Health Guide for the Care and Use of Laboratory Animals, approved by the Animal Ethics Committee of the Scientific Investigation Board of Shandong First Medical University.

Patient consent for publication

Not applicable.

Competing interests

The authors declare that they have no competing interests.

References

1. Hilliam Y, Kaye S and Winstanley C: *Pseudomonas aeruginosa* and microbial keratitis. J Med Microbiol 69: 3-13, 2020.
2. O'Callaghan R, Caballero A, Tang A and Bierdeman M: *Pseudomonas aeruginosa* Keratitis: Protease IV and PASP as Corneal Virulence Mediators. Microorganisms 7: E281, 2019.
3. Deng QC, Deng CT, Li WS, Shu SW, Zhou MR and Kuang WB: NLRP12 promotes host resistance against *Pseudomonas aeruginosa* keratitis inflammatory responses through the negative regulation of NF-κB signaling. Eur Rev Med Pharmacol Sci 22: 8063-8075, 2018.
4. Jang HH: Regulation of protein degradation by proteasomes in cancer. J Cancer Prev 23: 153-161, 2018.
5. Chen ZJ and Sun LJ: Nonproteolytic functions of ubiquitin in cell signaling. Mol Cell 33: 275-286, 2009.
6. Xu P, Duong DM, Seyfried NT, Cheng D, Xie Y, Robert J, Rush J, Hochstrasser M, Finley D and Peng J: Quantitative proteomics reveals the function of unconventional ubiquitin chains in proteasomal degradation. Cell 137: 133-145, 2009.
7. Guo L, Kong Q, Dong Z, Dong W, Fu X, Su L and Tan X: NLRC3 promotes host resistance against *Pseudomonas aeruginosa*-induced keratitis by promoting the degradation of IRAK1. Int J Mol Med 40: 898-906, 2017.
8. Guo L, Dong W, Fu X, Lin J, Dong Z, Tan X and Zhang T: Tripartite motif 8 (TRIM8) positively regulates pro-inflammatory responses in *Pseudomonas aeruginosa*-induced keratitis through promoting K63-linked polyubiquitination of TAK1 protein. Inflammation 40: 454-463, 2017.
9. Reyes-Turcu FE, Ventii KH and Wilkinson KD: Regulation and cellular roles of ubiquitin-specific deubiquitinating enzymes. Annu Rev Biochem 78: 363-397, 2009.
10. Love KR, Catic A, Schlieker C and Ploegh HL: Mechanisms, biology and inhibitors of deubiquitinating enzymes. Nat Chem Biol 3: 697-705, 2007.
11. Melo-Cardenas J, Zhang Y, Zhang DD and Fang D: Ubiquitin-specific peptidase 22 functions and its involvement in disease. Oncotarget 7: 44848-44856, 2016.
12. Yang M, Liu YD, Wang YY, Liu TB, Ge TT and Lou G: Ubiquitin-specific protease 22: A novel molecular biomarker in cervical cancer prognosis and therapeutics. Tumour Biol 35: 929-934, 2014.
13. National Research Council Committee for the Update of the Guide for the C and Use of Laboratory A: The National Academies Collection: Reports funded by National Institutes of Health. In: Guide for the Care and Use of Laboratory Animals. National Academies Press (US) Copyright© 2011, National Academy of Sciences, Washington (DC), 2011.
14. Chen K, Yin L, Nie X, Deng Q, Wu Y, Zhu M, Li D, Li M, Wu M and Huang X: β-catenin promotes host resistance against *Pseudomonas aeruginosa* keratitis. J Infect 67: 584-594, 2013.
15. Livak KJ and Schmittgen TD: Analysis of relative gene expression data using real-time quantitative PCR and the 2(-Delta Delta C(T)) Method. Methods 25: 402-408, 2001.
16. Hazlett LD: Pathogenic mechanisms of *P. aeruginosa* keratitis: A review of the role of T cells, Langerhans cells, PMN, and cytokines. DNA Cell Biol 21: 383-390, 2002.
17. Zhang Q, Lenardo MJ and Baltimore D: 30 Years of NF-κB: A blossoming of relevance to human pathobiology. Cell 168: 37-57, 2017.
18. Berger EA, McClellan SA, Barrett RP and Hazlett LD: VIP promotes resistance in the *Pseudomonas aeruginosa*-infected cornea by modulating adhesion molecule expression. Invest Ophthalmol Vis Sci 51: 5776-5782, 2010.
19. Ciornei CD, Novikov A, Beloin C, Fitting C, Caroff M, Ghigo JM, Cavaillon JM and Adib-Conquy M: Biofilm-forming *Pseudomonas aeruginosa* bacteria undergo lipopolysaccharide structural modifications and induce enhanced inflammatory cytokine response in human monocytes. Innate Immun 16: 288-301, 2010.
20. Chen K, Fu Q, Liang S, Liu Y, Qu W, Wu Y, Wu X, Wei L, Wang Y, Xiong Y, *et al*: Stimulator of interferon genes promotes host resistance against *Pseudomonas aeruginosa* keratitis. Front Immunol 9: 1225, 2018.
21. Hayden MS and Ghosh S: Shared principles in NF-kappaB signaling. Cell 132: 344-362, 2008.
22. Oh JY, Choi H, Lee RH, Roddy GW, Ylöstalo JH, Wawrousek E and Prockop DJ: Identification of the HSPB4/TLR2/NF-κB axis in macrophage as a therapeutic target for sterile inflammation of the cornea. EMBO Mol Med 4: 435-448, 2012.

23. Wang F, Jiang Z, Li Y, He X, Zhao J, Yang X, Zhu L, Yin Z, Li X, Wang X, *et al*: Shigella flexneri T3SS effector IpaH4.5 modulates the host inflammatory response via interaction with NF-κB p65 protein. Cell Microbiol 15: 474-485, 2013.
24. Yin J, Huang Z, Xia Y, Ma F, Zhang LJ, Ma HH and Li Wang L: Lornoxicam suppresses recurrent herpetic stromal keratitis through down-regulation of nuclear factor-kappaB: An experimental study in mice. Mol Vis 15: 1252-1259, 2009.
25. Glinsky GV, Berezovska O and Glinskii AB: Microarray analysis identifies a death-from-cancer signature predicting therapy failure in patients with multiple types of cancer. J Clin Invest 115: 1503-1521, 2005.
26. Glinsky GV: Genomic models of metastatic cancer: Functional analysis of death-from-cancer signature genes reveals aneuploid, anoikis-resistant, metastasis-enabling phenotype with altered cell cycle control and activated Polycomb Group (PcG) protein chromatin silencing pathway. Cell Cycle 5: 1208-1216, 2006.
27. Zhao Y, Lang G, Ito S, Bonnet J, Metzger E, Sawatsubashi S, Suzuki E, Le Guezennec X, Stunnenberg HG, Krasnov A, *et al*: A TFTC/STAGA module mediates histone H2A and H2B deubiquitination, coactivates nuclear receptors, and counteracts heterochromatin silencing. Mol Cell 29: 92-101, 2008.